Position dependence of the performance gain by selective ground albedo enhancement for bifacial installations

Nils-Peter Harder[1], Issam Smaine[1], Fadi Bourarach[1], Damien Cosme[2], Ines Arfaoui[1], Julien Chapon[1], Arttu Tuomiranta[1], and Antonios Florakis[1,3]

[1]TotalEnergies, 91120 Palaiseau, France

[2]TotalEnergies Research Center Qatar, Qatar Science and Technology Park, P.O. Box 9803 – Doha – Qatar

[3]Advanced Solar Energy Technologies Consulting BV, 3000 Leuven, Belgium

2023 IEEE 50th Photovoltaic Specialists Conference (PVSC) | 978-1-6654-6059-0/23/$31.00 ©2023 IEEE | DOI: 10.1109/PVSC48320.2023.10359920

***Abstract* — We explore how positioning high-albedo material on the ground impacts the performance gain obtainable by these selective ground albedo enhancements. The ground albedo can be improved, for example, by placing geosynthetic materials, white stones, or paint under or between PV panels. Specifically, we determine how the most effective positioning of albedo enhancement material (AEM) is influenced by geographic latitude, by the diffuse-light content in the total irradiance, by the choice between tracking versus fixed-tilt mounting, and by module mounting height. We find for fixed-tilt systems that albedo improvement strips with a width similar to the module table or less, should be under the tables, but shifted towards the sun-facing leading (lower) edge of the modules. This preference for placement towards the lower edge is slightly more pronounced the closer the location is to the equator. For typical / high-mounted (1.5m torque-tube height) tracked systems, for all albedo strip widths, the optimum placement is centered at the center of the module table. However, for low-mounted tracked systems and a ground area coverage by the AEM of about equal or less the module table width, we find that it is favorable to split the material into two off-centric strips rather than one strip centered to the trackers. Interestingly, we find for both fixed-tilt and tracking systems that the optimum placement of such albedo enhancement strips is not notably influenced by the diffuse content of the irradiation. However, the magnitude of the gain is influenced by the diffuse content and we find higher relative gain from albedo improvement in case of a high diffuse light content. Particularly for tracked systems the relative production gain by ground albedo enhancement is larger for higher diffuse content. Of course, the overall performance of tracked systems prefers low diffuse light content and dominance of DNI.**

I. Introduction

Bifaciality of photovoltaic (PV) modules has notably contributed to driving down PV electricity generation cost, and large utility power plants (UPPs) are these days increasingly designed as bifacial installations [1]. Compared to monofacial installations, a bifacial system favors higher module racking (and wider row-to-row spacing), to allow more light under the modules and more efficient back-reflection from the ground onto the rear sides of the modules. Another option for improving the bifacial gain of a PV system is to change the properties of the ground. This can involve placing white gravel, geotextiles, or paint on the ground under or between the modules [2], [3]. Such ground albedo improvement is cheaper per area than the module cost per area, yet the cost of such ground improvement can be a notable factor in the total system cost. Because different positions on the ground are differently efficient for reflecting sunlight back onto the rear sides of the panels, it can be economically beneficial to apply the albedo improvement only on parts of the ground. Albedo is very often to a good degree of approximation Lambertian (that is: angle-independent radiant reflection intensity for all directions). Generally, ground areas closer to the modules reflect incoming light more efficiently back onto the modules (unless view factor effects minimize the radiation transfer, such as for ground areas underneath vertically mounted panels). At the same time, the ground areas closest to the modules, for example directly under the modules of a fixed-tilt installation, may receive less light to reflect at all, because these regions will be more frequently shaded by the modules (see Fig. 1). It is therefore a non-trivial optimization task to define the best placements for ground albedo improvement.

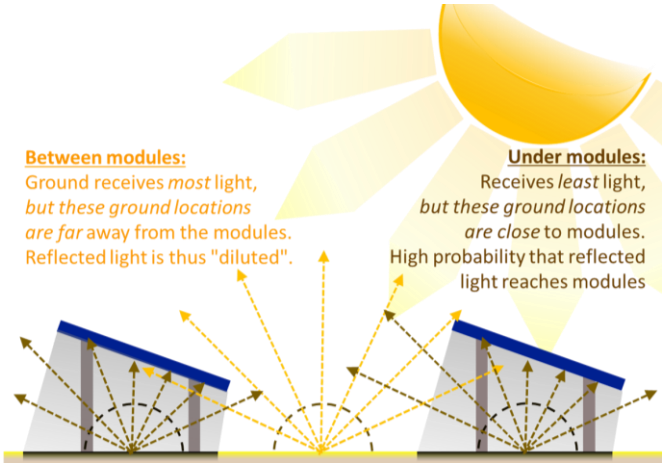

Fig. 1. Optimization problem for placement of albedo enhancement material that covers less than 100% of the ground area. Ground areas that receive most sunlight are far from modules, and vice versa.

Jaubert *et al*. [2] and Rhazi *et al*. [3] already explored several configurations of albedo enhancement materials (AEM) under PV modules in bifacial solar systems. In our study, we provide a systematic investigation on the dependence of the obtainable

gain on the position of the ground albedo improvement on flat ground. Mandy Lewis presented at this conference, where our work was presented, too, highly related results [4]. We highlight general effects of several parameters on this position dependence for partial (or "selective") ground albedo improvement. In particular, we investigate the effect of latitude, diffuse-light content in the solar irradiance, and module mounting height. We explore these effects for single-axis tracking systems as well as for fixed-tilt systems.

While any project will profit from dedicated simulations of the best placement for albedo improvement, our study allows us to estimate the main effects for a wide range of situations.

II. Simulation Model

We use SolarOPS PV system performance simulation software [5], developed by TotalEnergies. SolarOPS incorporates both ray-tracing (RT) and view-factor (VF) optical engines, which are based on various open-source modules from PV Performance Modeling Collaborative [6]-[8] and Radiance [8]. We radically re-designed parts of these modules to add several additional features that enable us to model specific complex scenarios. One of these additional features relevant for this work is the ability to set zones of differentiated albedo also in the VF model, instead of having only a uniform albedo distribution. Strips of material with increased albedo can be placed on various positions and with various widths between or under the two module rows, allowing for the optimization of the strip placement. (For the RT version, this functionality is intrinsically available as RT allows direct assignment of the optical properties of the different zones of the scene.) Via RT, it is possible to include the impact of the racking and torque tube geometry and its shading, and thus it is more suitable for detailed simulation studies and often necessary for simulating small R&D test installations, while the typical implementation of VF models only represent systems with long rows of modules where edge effects can be neglected [9]. On the other hand, the current implementation of RT in SolarOPS is computationally demanding and, therefore, not as practical for large-scale optimization studies. For this purpose, we often opt in such cases for the much faster VF-based modeling. The main limitation of VF is the neglection of said edge effects [10] due to the implicit assumption of semi-infinite module table rows. We show in our validation example in section III that this neglection/idealization of VF diminishes with increased length of the module rows and that VF is therefore suitable for simulating UPP scenarios.

We use astronomic tracking with backtracking in the simulations presented in this paper.

III. Model Validation

Our R&D team, based in Palaiseau, France and Doha, Qatar, studies module and PV system performance at various installation locations across the world. By comparing simulation results to production data from various R&D PV test installations and UPPs and also by doing "peer-to-peer" comparison with e.g., PVsyst, we validate and improve our system simulation software SolarOPS continuously. This section of our paper reports on a comparative study for two R&D systems in Doha, thanks to our collaboration with the Qatar Environment and Energy Research Institute (QEERI). Both systems are installations of 2x3 half-cell modules, and one of them features a geomembrane for improved albedo on a section of the ground (Fig. 2).

Fig. 2. Photo of experimental PV test-stand, used in this study as an example-validation case, representing regular other validations of our model. In this study, we compare the energy yield of this set-up against an identical system without artificial ground albedo enhancement.

Fig. 3 shows data from these systems, comparing the experimental observations to RT and VF modelling. RT modelling closely reproduces the experimentally observed energy gain from improving the ground albedo with a geomembrane. VF-based modelling is not precise for small systems [10], but converges with more accurate RT modelling for longer rows of modules (Fig. 3); the latter represents the case of UPPs that we address in the main section of this paper.

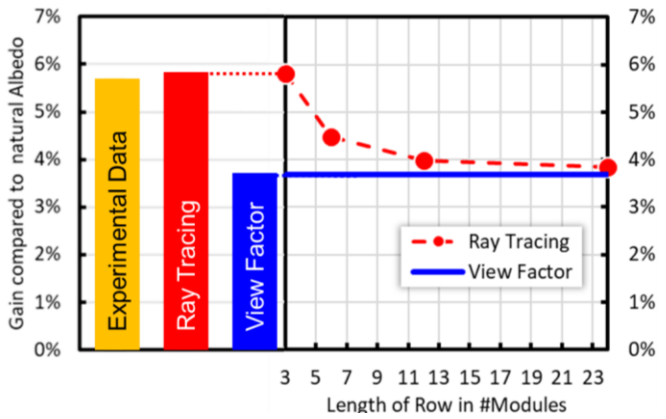

Fig. 3. Left: Measured and simulated energy yield gains from artificial ground albedo improvement. Right: View-Factor-based simulation converges with more accurate Ray-Tracing for long module rows typical of UPP installations.

IV. Definition of Systems for Albedo Study

Using VF modeling, we simulate systems in Doha, Qatar, and Toulouse, France, with 6.5m row-to-row pitch and a ground-coverage ratio (GCR) of 32.6% with 2.12m-long modules in portrait orientation. The modules in these simulations are Jolywood D72N 410 Monocyrstalline Silicon, with a bifaciality factor of 80%. The corresponding PAN file was exported from PVsyst [11, 12]. The inverter in this study was represented by an OND file for the inverter UEP-4700 of Gamesa.

Our study has the aim to determine the best positions on the ground where to place high-albedo material, to achieve the highest production gain for a given amount of AEM placed on the ground. We approach this purpose by first presenting simulation results that are free of clipping effects. Specifically, we used a DC/AC ratio of 0.84, that is 73 383 kWp DC, with a total AC capacity of the inverters of 87 106 kWp. After determining clipping-free ("real") ground position sensitivity to albedo enhancement, we discuss the effect of clipping on the shape of such ground sensitivity curves.

Figure 4 illustrates how these sensitivity curves are constructed, comparing the gain achieved by strips of enhanced ground albedo to the operation of the same system with only natural albedo.

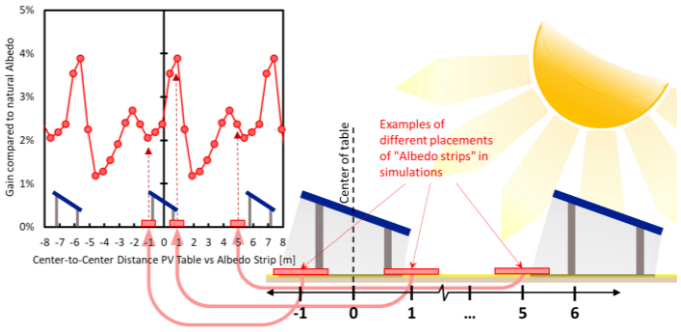

Fig. 4. Schematic representation of a bifacial PV system on the right, with examples of different placement options of albedo enhancement material on the ground. The arrows point to the corresponding x-axis values of a graph that plots the gain created by the AEM on the ground as a function of the placement position, and compared to operating the system with only natural ground albedo.

In the fixed-tilt cases, we use an inclination angle of 22° for Doha and 32° for Toulouse. Other than the inclination angles, latitudes, and meteorological data, we use the same system definitions in Doha and in Toulouse, with a natural ground albedo of 20% and for the areas with artificial ground albedo enhancement we use an albedo value of 75%.

The tracking systems follow an astronomical tracking algorithm, with a limiting angle of 60° and backtracking.

The center heights of the module tables in the tracked cases and in the fixed-tilt cases are 1.1m and 1.5m. For tracked installations this corresponds essentially to the torque-tube height. For fixed-tilt cases, one typically specifies the "ground clearance" i.e., the distance between the lower ("leading") edge

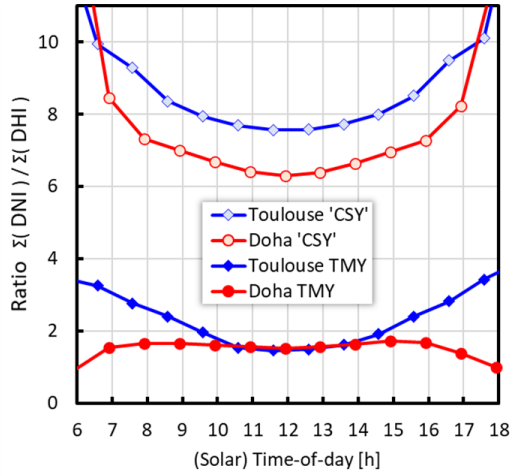

Fig. 5. Ratio of the annual sum of DNI, and sum of the annual DHI plotted for each hour of the day. Shown are results for the four meteo files used in the simulation study: TMY data for Toulouse and Doha, and "clear-sky-years" (CSY) in the same locations, where the CSY is an artificially created meteo file consisting of only clear-sky days.

of the modules and the ground. Since we are using (according to the different latitudes) different mounting angles in Doha and in Toulouse, the same center heights imply different ground clearances. We chose to keep the same center height, as to provide a more direct comparison of the optical configuration between the fixed-tilt cases in Doha and Toulouse, and a more direct comparison to the tracked cases.

Please also note that a "one-portrait" configuration is unusual for fixed-tilt installations. Again, this choice was made to have a more direct comparison between the tracked and the fixed-tilt cases. The fixed-tilt results remain applicable to other cases (such as "two-portrait") by noting that performance of the "one-portrait" case is identical to the performance of a "two-portrait" case, if the center height and row-to-row spacing is scaled accordingly i.e., by a factor of "2".

In order to explore the effect of the content of the diffuse light and the direct light on the ground sensitivity curves that were sketched in Fig. 4, we generated for both locations, Doha and Toulouse, "clear-sky years" (CSY). To this end, we used a function in PVsyst [12] that allows for a given location to construct meteorological data where each day of the year is a clear-sky day. Figure 5 provides an impression on the relative amount of direct light compared to diffuse light, as a function of the hour of the day, shown for regular typical meteorological year (TMY) files for Toulouse and Doha and for the corresponding CSY artificial meteo data. Also seen in Fig. 5 are slight asymmetries for times before and after "solar noon", leading in our simulation results to corresponding slight asymmetries for the albedo ground sensitivity curves. Note that otherwise for north-south-oriented single-axis tracker systems the ground sensitivity curves would be perfectly symmetric in a climate where morning irradiance matches the afternoon irradiance.

V. Results

Figure 6 shows our simulation results for the fixed-tilt systems in the two different locations, Doha and Toulouse. Each data point on the curves represents a simulation of a full year, either a TMY as indicated by the closed symbols, or a year with only clear-sky days (calculated from the TMY), indicated as open symbols in the graph. The *x*-axis value of each data point refers to the position of the strip of improved albedo that was used in the simulation (compare to Fig. 4). We can see that for fixed tilt systems, the best position for narrow strips (equal or less than the module table width) is to center the strip near the front (sun-facing lower edge) side of the module row. For albedo strips that are wider than the module table, the optimum position shifts to the rear side (higher edge) of the module row. This observation holds true for both module mounting heights: Indicated in the graph are the heights of the center of the module table above ground.

Interestingly, the use of a CSY as meteo input did not change the qualitative shapes of these ground sensitivity curves. However, as visible by the slightly different scale for the right axis for the open symbols, a more direct light content (CSY) creates less performance gain by ground albedo enhancement than under TMY conditions.

While some details of the graphs for Toulouse and Doha are different, the main conclusion about the design rules for placing ground enhancement materials is the same: For fixed-tilt systems, the best position for strips of albedo enhancement is

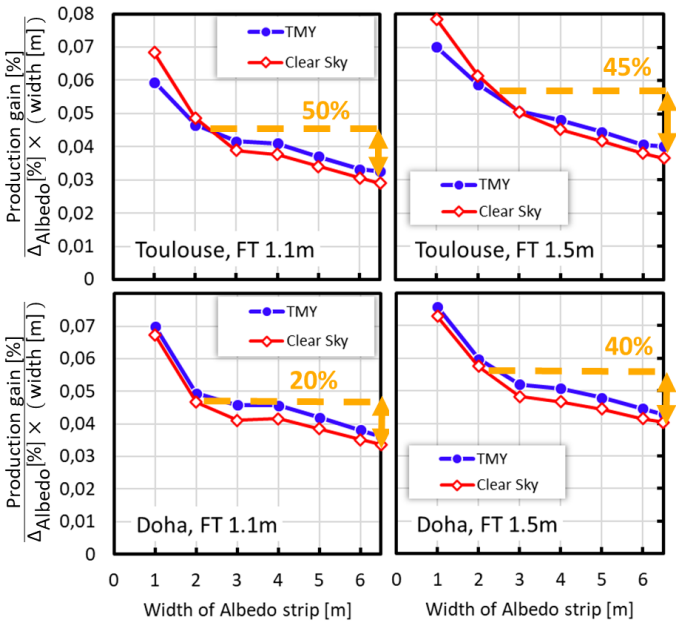

Fig. 7. The efficiency or "value" per area of the albedo enhancement material placed on the ground, plotted as a function of the width of optimally placed strips of AEM. The module bifaciality in these fixed-tilt (FT) simulations was 80%, and the curves scale accordingly for modules with a different bifaciality factor. The "value" per material for strip widths similar to the module table (2.12m here) can be up to 50% higher than for full-area ground coverage.

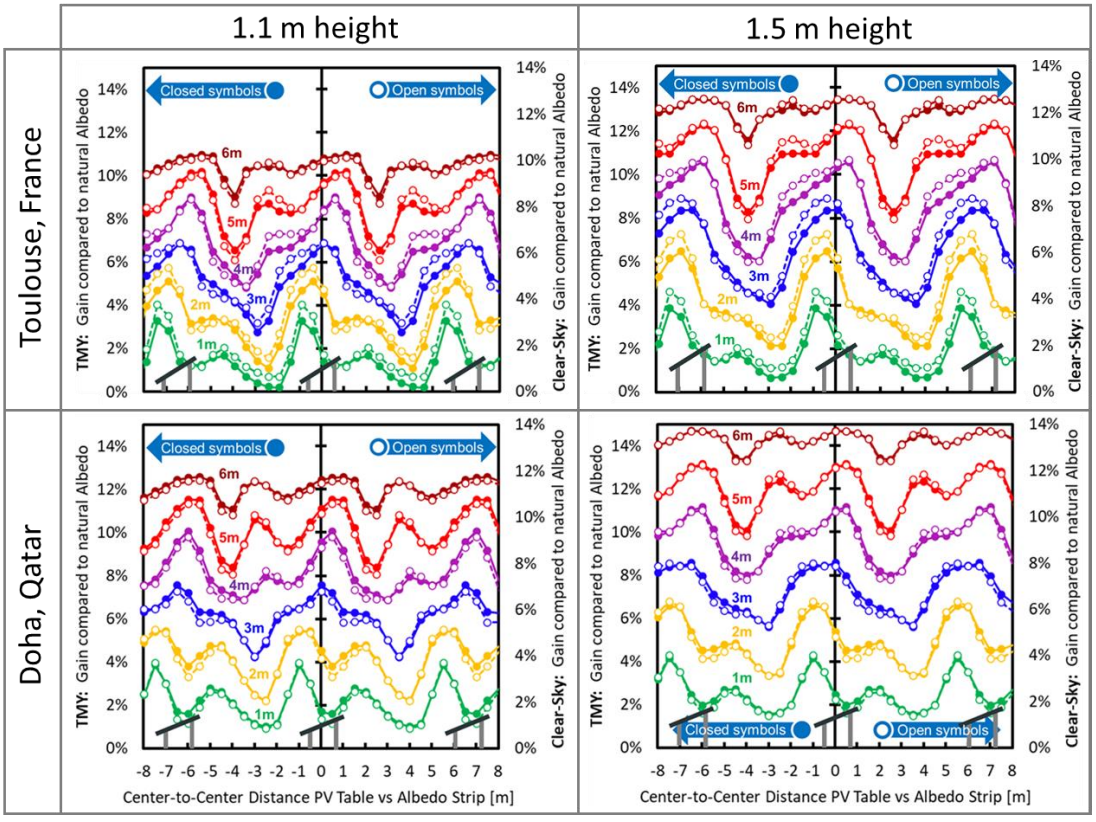

Fig. 6. Fixed-tilt energy production gain by arranging strips of enhanced albedo (75%) on the ground (20% albedo). Module bifaciality: 80%. Each graph shows results for six strip widths (1m to 6m), indicated next to curves. Horizontal axis indicates the position of albedo strips on the ground. Module racking schematically sketched (to scale) at bottom of each figure. Upper graphs: Toulouse. Lower graphs: Doha. Left graphs: center height 1.1m, right graphs: 1.5m. Left axes (all same scale) are for TMY (closed symbols). Right axes (all same scale, but different to left axis) are for the "clear-sky years" i.e., simulation results with artificial meteo files that have only clear-sky days.

near the lower edge of the module table in case the strip widths are comparable to the module table width or smaller. For wider strips, a position centered under the module table is preferred.

Figure 7 plots for all four fixed-tilt systems the obtainable performance gain versus the witdth of the albedo enhancement strip (red and blue curves). For each width of the strip, the optimum position was assumed. Note the quantity and units of the vertical y-axis: Gain versus "only natural albedo", divided by the difference (ΔAlbedo) between the natural albedo and the enhanced albedo value, and divided by the width of the albedo strip. Except for bifacility of the modules (here: 80%) this quantity divides the gain by those variables that can be expected to cause a proportional effect on the gain, and it therefore expresses in a generalized form how much gain can be expected "per meter (width) of invested AEM". The graphs show, that for an albedo strip of the width of the module table (here 2.12m) an optimized placement produces 20-50% more production gain "per invested meter width" than a full-area coverage with AEM.

Figures 8 and 9 show the same fashion as Figs. 6 and 7 the corresponding simulation results for tracked systems. Generally, we find for the SAT tracking systems ground sensitivity curves that are symmetrical to the center of the tracker torque tube. As a general rule-of-thumb, one can see that for SAT tracking systems, the most efficient placement of AEM is right under the tracker, centered to the torque tube. Again, the qualitative difference of the shapes of these curves is not much

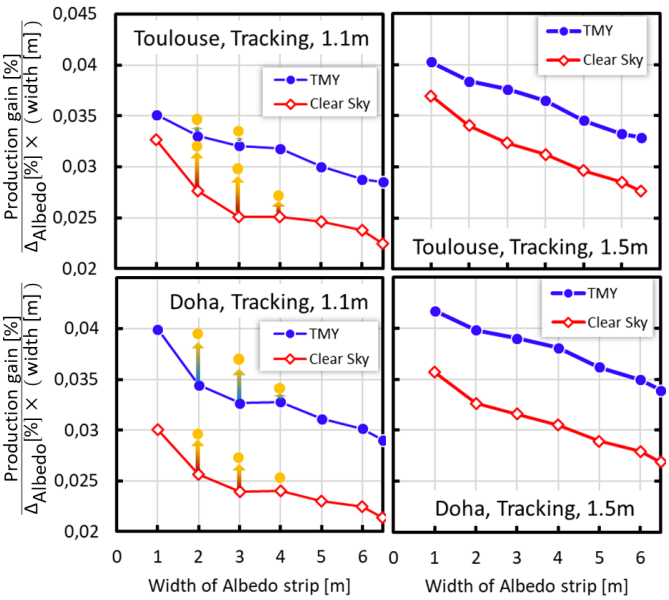

Fig. 9. Efficiency or "value" per area of the albedo enhancement material placed on the ground, plotted as a function of the width of optimally-placed strips of AEM. The module bifaciality in these SAT tracking simulations was 80%, and the curves scale accordingly for modules with a different bifaciality factor. The "value" per material can be increased (yellow points) if the material of the total strip width is divided into two narrower strips, placed off-centric to the tracker.

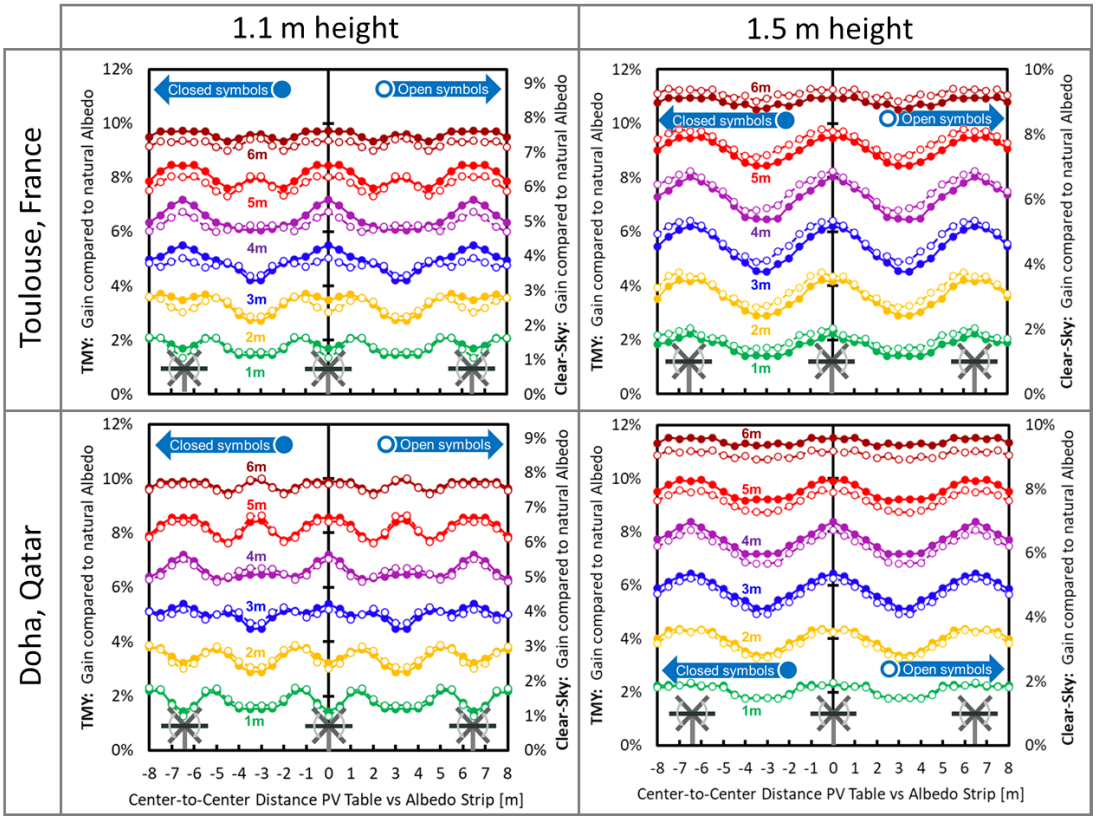

Fig. 8. Tracking system (SAT) energy production gain by arranging strips of enhanced albedo (75%) on the ground (20% albedo). Module bifaciality: 80%. Each graph shows results for six strip widths (1m to 6m), indicated next to curves. Horizontal axis indicates the position of albedo strips on the ground. Module racking schematically sketched (to scale) at bottom of each figure. Upper graphs: Toulouse. Lower graphs: Doha. Left graphs: center height 1.1m, right graphs: 1.5m. Left axes (all same scale) are for TMY meteo (closed symbols). Right axes (slightly different for left and right graphs) are for the "clear-sky years", i.e. simulation results with artificial meteo files that have only clear-sky days.

different between the more diffuse TMY meteo situation and the clear-sky DNI-dominated CSY meteo data. We do see, however, that for the tracked case, the relative gain obtainable for albedo enhancement is more pronounced for more diffuse light (compare y-axis units for the solid and the open symbols).

The other notable difference is the development of two peaks to the east and west of the torque tube position (with a minimum at the center) for 1m and 2m wide albedo strips for lowly-mounted tracked systems. This has a notable effect for the optimization of the placement of AEM: The yellow symbols in Fig. 9 indicate that placing material in the form of two narrower strips (instead of one wide strip) can use the invested material notably more efficiently for lowly-mounted tracking systems as one may encounter in more windy regions.

All of the results shown up to this point were generated in scenarios without clipping. While clipping does not change the general trends, it does reduce the relative gain obtainable by albedo enhancements, and also some of the finer details and optimization options found in the system. Figure 10 shows the effect of clipping for two example cases of the tracking scenarios: 1.5m center height with 3m AEM strip width, and 1.1m center height with 2m AEM strip width. Apart from a general lowering of the relative gain obtainable, we see a reduction of the finer features in the ground sensitivity curves for high degree of clipping. In particular, the two separate double-peaks for the lowly-mounted tracking systems vanish, so that the general rule that centering ground AEM centered under the tracker also re-emerges again for this case.

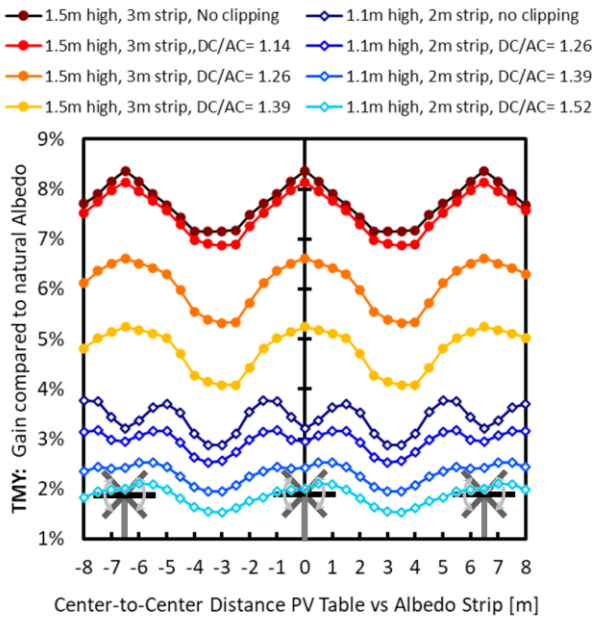

Fig. 10. Selected SAT tracking configurations from Fig. 8 (see graph legend, and compare to the non-clipped cases in Fig. 8) SAT Doha 1.1m height with 2m wide strip and Doha, 1.5m with 3m wide strip, to show the effect of clipping on the ground sensitivity curves for AEM placement.

VI. Conclusions

This paper presents the main effects of the positioning of albedo enhancement material (AEM) on the ground. In particular we have explored how the PV production gain by these AEM depends on where on the ground it is placed. In some cases up to 50% more gain per invested material on the ground can be achieved, when placing the AEM in the best positions only, as compared to a full-area ground coverage. We show these effects for tracking or fixed-tilt bifacial solar systems in different latitudes and climates. Our results allow deriving the general rule of thumb, that a positioning of AEM centered under the modules is optimal for AEM widths notably wider than the module table. For AEM strips of about the module table width (or less), fixed-tilt systems prefer centering the AEM near the lower (front) edge of the module table. For tracked systems with a low mounting height, it can be beneficial to split the AEM into two off-center strips to east and west of the SAT tracker.

References

[1] R. Kopecek, J. Libal, "Bifacial Photovoltaics 2021: Status, Opportunities and Challenge", *Energies* vol. 14, p. 2076, (2021).

[2] J.-N. Jaubert, Yuanjie Yu, Baohua He, Gang Yan, Zhigen Zhang, Ray Zhao, "Layout optimization of Albedo enhancer materials used in bifacial PV systems," *6th BiFi PV Workshop*, 2019.

[3] O. Rhazi, M. Chiodetti, J. Dupuis, S. Benyakhlef, K. Radouane, P. Dupeyrat, "Optimizing the utilization of reflective materials for bifacial PV plants," *37th EU-PVSEC*, 2020, p.1286.

[4] "Energy Yield and Economics of Single-Axis-Tracked Bifacial Photovoltaics with Artificial Ground Reflectors", M.R. Lewis, S. Ovaitt, B. McDanold, C. Deline, K. Hinzer. Presented at this same conference: 50th IEEE-PVSC (2023)

[5] A. Florakis, F. Bourarach, E. Houzay, N.-P. Harder, I. Smaine, A. Poquet, A. Buzy-Debat, S. Ait-Tilat, J. Chapon, P. Biver, T. Chugunova, A. Tuomiranta, and G. Poulain (2023, May 9). SolarOPS: A versatile PV system simulation software. 16th PV Performance Modeling Workshop, Salt Lake City, Utah, USA. https://www.sandia.gov/app/uploads/sites/243/2023/06/5-6_PVPMC23-SolarOPS-Gen2-final-1.pdf

[6] W. F.. Holmgren, C. W. Hansen, and M. A. Mikofski. "pvlib python: a python package for modeling solar energy systems," *Journal of Open Source Software*, 3(29), P. 884, (2018).

[7] B. Marion, S. MacAlpine, C. Deline, A. Asgharzadeh, F. Toor, D. Riley, J. Stein, and C. Hansen, "A Practical Irradiance Model for Bifacial PV Modules," *44th IEEE Photovoltaic Specialists Conference*, pp. 1537-1542, (2017).

[8] S. A. Pelaez, and C. Deline, "bifacial_radiance: a python package for modeling bifacial solar photovoltaic systems," *Journal of Open Source Software*, 5(50), p. 1865, (2020)

[9] G. W. Larson, and R. A. Shakespeare, "Rendering with Radiance: The Art and Science of Lighting Visualization", San Francisco: Morgan Kaufmann Publishers, Inc. (1998)

[10] S. A. Pelaez, C. Deline, S. M. MacAlpine, B. Marion, J. S. Stein, and R. K. Kostuk, "Comparison of Bifacial Solar Irradiance Model Predictions With Field Validation," in *IEEE Journal of Photovoltaics*, vol.9(1), pp. 82-88, Jan. 2019.

[11] A. Mermoud, "PVSYST: a user-friendly software for PV-systems simulation", Proceedings of 12th EU-PVSEC 1994, p. 1703

[12] https://www.pvsyst.com/